A seat suspension with a rotary magnetorheological damper for heavy duty vehicles

2016 Smart Mater. Struct. 25 105032

(http://iopscience.iop.org/0964-1726/25/10/105032)

IOP Publishing Smart Materials and Structures
Smart Mater. Struct. 25 (2016) 105032 (10pp) doi:10.1088/0964-1726/25/10/105032

A seat suspension with a rotary magnetorheological damper for heavy duty vehicles

S S Sun[1], D H Ning[2], J Yang[1], H Du[2], S W Zhang[3] and W H Li[1]

[1] School of Mechanical, Materials and Mechatronic Engineering, University of Wollongong, New South Wales 2522, Australia
[2] School of Electrical, Computer & Telecommunications Engineering, University of Wollongong, New South Wales 2522, Australia
[3] Department of Precision Machinery and Precision Instrumentation, University of Science and Technology of China, Hefei, Anhui province 230026, People's Republic of China

E-mail: weihuali@uow.edu.au and swzhang@ustc.edu.cn

Received 29 May 2016, revised 21 July 2016
Accepted for publication 18 August 2016
Published 26 September 2016

Abstract

This paper presents the development of an innovative seat suspension working with a rotary magnetorheological (MR) fluid damper. Compared with a conventional linear MR damper, the well-designed rotary MR damper possesses several advantages such as usage reduction of magnetorheological fluid, low sealing requirements and lower costs. This research starts with the introduction of the seat suspension structure and the damper design, followed by the property test of the seat suspension using an MTS machine. The field-dependent property, amplitude-dependent performance, and the frequency-dependent performance of the new seat suspension are measured and evaluated. This research puts emphasis on the evaluation of the vibration reduction capability of the rotary MR damper by using both simulation and experimental methods. Fuzzy logic is chosen to control the rotary MR damper in real time and two different input signals are considered as vibration excitations. The experimental results show that the rotary MR damper under fuzzy logic control is effective in reducing the vibrations.

Keywords: seat suspension, rotary MRF damper, vibration control

(Some figures may appear in colour only in the online journal)

1. Introduction

Prolonged periods of time spent in a vibrating machine causes the hazard known as whole-body vibration or WBV. Vibration transferred from uneven road surfaces, vibrating tools, and vibrating machinery to a vehicle driver's body significantly influences drivers' comfort and safety. Long term exposure to high levels of WBV can also cause physical pain in the driver's neck/shoulders, lower back injuries, spinal injuries, and other musculoskeletal diseases, not only while driving but during their off time as well, and is becoming a major problem [1]. The WBV problem is much more serious in the mining industry, construction field and agriculture because rough road conditions can cause fierce vibration to vehicles or heavy machines (bulldozers, shearers, etc) and the suspension of heavy machines and trucks used in the above areas must stiffen enough to carry their weight. The hard suspension, however, makes the vibrations caused by uneven roads and the operating actions of heavy vehicles easily transmitted to the body and this causes the drivers to experience an uncomfortable ride and ultimately, suffer health problems. Long term exposure to WBV can cause workers permanent health problems such as numbing of nerves, gut problems, spinal injuries and damage to a woman's ability to conceive [2, 3].

The aim of this paper is to investigate ways of protecting the workers from such unhealthy and unsafe working routines by arming the heavy machinery and trucks with advanced seat suspensions. Seat suspension has been adopted in vehicles, particularly used for commercial industry, mining,

agriculture, and transport purposes [4, 5], to provide the drivers with ride comfort, to reduce the fatigue due to long hours of driving or exposure to severe working environments, and to improve the safety and health standards. The optimisation and control of seat suspensions for vertical vibration reduction has been an active research topic for decades. To date, passive [6], active [7–9] and semi-active [3, 10, 11] seat suspensions have been proposed. A passive seat suspension is simple, reliable, and cost-effective but it cannot provide a controllable force and consequently, performance is inevitably limited. While maintaining the geometric and dynamic properties of a passive suspension structure, an active or semi-active device has been considered for incorporation in modern seat suspension structures to meet the requirements. In particular, semi-active seat suspensions offer performance comparable to that brought by active seats without requiring high power consumption and expensive hardware. In the past decades, magnetorheological fluid (MRF) has been the preferred choice to make semi-active devices realistic [12–14]. MRF is very responsive to magnetic field, with an estimated response time of less than 10 ms [15], and requires relatively low power to operate [16, 17]. Semi-active seat suspensions founded on MR dampers have begun to be investigated and have achieved certain expectations. For example, Choi and Han [11, 18] applied MR dampers to attenuate the vertical seat vibration. Choi and Wereley [19] investigated the application of MR dampers to helicopter crew seats to enhance the survivability of a crash. Bai and Wereley [20] extended their work on the application of MR seat suspension for mitigating ground vehicle crashes. The current MR dampers have all been linear dampers with inherent drawbacks which need to be addressed: (1) in principle, high pressure inside damper is always needed to avoid the force lag performance, which require advanced sealing technology for the avoidance of fluid leakage; (2) With respect to the usage of MRF, the reserve of the linear damper must be totally filled up, which results in higher consumption of the MRF material and high cost. For the above reasons, there is great possibility to advance the current seat suspension design by overcoming the above-mentioned requirements.

In order to reduce the requirements of a conventional seat suspension with linear dampers, this paper proposes a new seat suspension structure using a rotary MR damper. The seat suspension with a linear MR damper has been widely investigated but the research on semi-active seat suspension utilising a rotary MR damper is very rare. Compared with conventional seat suspension with a linear MR damper, which needs large amounts of MR fluids to fill the reserve of the linear MR damper, a rotary damper based seat suspension only utilizes a smaller quantity of MRF because the reserve of the rotary MR damper is much smaller than that of a linear one. This advantage significantly reduces the cost of the seat suspension [21]. Another advantage over linear dampers is the lack of need for sealing the rotary MR damper. The working mechanism of the linear MR damper relies on the pressure difference between the two sides of the piston, which means the pressure of at least one side is quite high and thus needs good sealing. In terms of the rotary MR damper, the working mechanism is different and the MRF pressure is quite low, thus it is much easier to solve the sealing problem. The advantages of compact structure, anti-sedimentation of MR fluids and easy assembly of rotary MR dampers should also be noted.

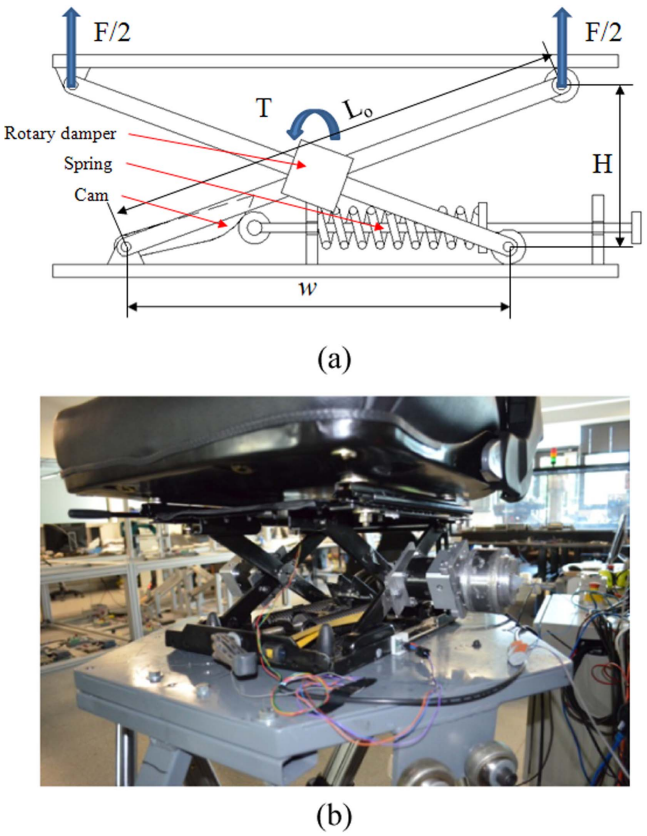

Figure 1. The structure of the seat suspension: (a) working mechanism; (b) photograph of the suspension system.

For these reasons, the development of a rotary MR damper for heavy duty vehicles aims at upgrading the current seat suspension technology and improving the ride comfort of drivers. The specific contents of this paper are introduced as follows. Following the introduction, the structure and design of the proposed seat suspension will be presented. The property test of the seat suspension will be conducted in section 3 and the test results will be discussed. Sections 4 and 5 present the vibration attenuation performance of the seat suspension numerically and experimentally, respectively. The conclusion is drawn in section 6.

2. The structure and design of the seat suspension

2.1. The structure of the seat suspension with rotary MR damper

Figure 1 shows the structure of the proposed seat suspension system which is mainly composed of the scissors structure with rotary MR damper installed. One beam of the scissors structure is fixed with the shaft of the damper and the other is fixed with the outside cylinder. When this seat intends to

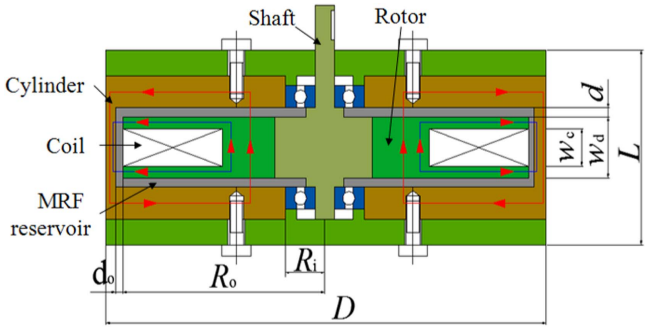

Figure 2. The structure of the rotary MR damper.

vibrate vertically, the relative motion of these two crossed beams will drive the rotary damper to work. In this way, the vertical linear movement is transformed into rotational motion of the rotary dampers. Subsequently, the damping variation of the rotary MR damper will induce the overall damping variation of the seat suspension.

2.2. The design of the rotary MR damper based seat suspension

The design of the seat suspension, including its structure and peak force, is important for the seat to achieve better ride comfort. Specifically, the structure of the seat suspension should be compact and the maximum force of the MR damper should be able to emulate the maximum desired control force that occurs under worst-case base disturbance. This subsection presents the design and peak force calculation procedure for the seat suspension in order to provide a design guideline.

Figure 2 shows the structural design of the proposed rotary MR damper. In general, it can be seen that this rotary MR damper consists mainly of a cylinder, a coil, a shaft, a rotor, and the enclosed reservoir filled with MRF. Unlike the linear MR damper with single shaft, the rotary MR damper does not need a spring or gas chamber to provide the initial pressure in the damper. The rotor is made of low-carbon steel and the shaft is made of aluminium. The choice of material for different parts is under the consideration of magnetic circuit design. The coil is composed by winding the copper wire around the rotor. When the coil is energized, two sets of magnetic circuits are formed as shown in figure 2. This magnetic circuit design guarantees that the magnetic flux passes through the MRF.

The peak torque is the most important index for the rotary MR damper design and directly determines the ride comfort of the seat suspension. The calculation method is shown as follows [22]:

$$T_\tau = \frac{4\pi\mu_{eq}R_o^4}{(n_e+3)d}\left[1-\left(\frac{R_i}{R_o}\right)^{n_e+3}\right]\Omega + \frac{4\pi\tau_{ye}}{3}(R_o^3-R_i^3) + 2\pi R_o^2 L_a\left(\tau_{ya}+K_a\left(\frac{\Omega R_O}{d_o}\right)^{n_a}\right), \quad (1)$$

Table 1. The size of the rotary MR damper.

d_o	1.5 mm	w_c	22 mm
R_o	34 mm	w_d	12 mm
R_i	20 mm	L	45 mm
D	100 mm	d	1.5 mm

Table 2. The parameters for the MRF-132DG.

K_O	0.22 Pa s^n	$\tau_{y\infty}$	30 000 Pa
K_∞	3900 Pa s^n	α_{sty}	2 T^{-1}
α_{sk}	5 T^{-1}	n_O	0.917
τ_{yO}	10 Pa	n_∞	0.25
α_{sn}	32		

$$T_{\tau o} = \frac{4\pi\mu_{eqo}R_o^4}{(n_o+3)d}\left[1-\left(\frac{R_i}{R_o}\right)^{n_o+3}\right]\Omega + \frac{4\pi\tau_o}{3}(R_o^3-R_i^3) + 2\pi R_o^2 w_d(\tau_o+K_o\left(\frac{\Omega R_O}{d_o}\right)^{n_o}), \quad (2)$$

where T_τ is the torque with magnetic field and $T_{\tau o}$ is the torque without magnetic field. τ_{ye}, K_e, and n_e, are yield stress, the consistency and the behaviour index of the MRF in the end-face duct. μ_{eq}, governed by $\mu_{eq} = K_e\left(\frac{R_o\Omega}{d}\right)^{n_e-1}$, is the equivalent viscosity of the MRF in the end-face duct. $L_a \cong w_d - w_c$ is the effective length of the annular duct. The meanings of d, D, L, d_o, R_o, R_i, w_c and w_d have been given in figure 2. The detailed size of the rotary damper is shown in table 1. According to the size, the MRF usage for the rotary damper can be calculated, which is 13.87 ml. As a comparison, the MRF usage in a representative paper [3] using a linear MR damper for seat suspension is approximately 126.24 ml. The MRF usage in the rotary damper designed in this paper is significantly less.

Based on the reference [23], the rheological properties of the MRFs can be estimated by the following equation:

$$Y = Y_\infty + (Y_o - Y_\infty)(2e^{-B_{o}\alpha_{SY}} - e^{-2B_{o}\alpha_{SY}}), \quad (3)$$

where Y represents rheological properties of MRF including post-yield viscosity, yield stress, fluid consistency, and flow behaviour index. The value of the MRF rheological properties Y has a range of Y_o (zero applied field) to Y_∞ (saturation value). B is the applied magnetic flux density and can be calculated by finite element analysis method. α_{SY} is the saturation moment index. Based on the curve fitting results with experimental results, the values of Y, Y_∞ and α_{SY} corresponding to different rheological properties of MRF (LORD MRF-132DG) can be determined and they are given in table 2. Subsequently, the peak torque of the rotary MR damper under 0 A current and 1 A current can be calculated: $T_{\tau o} = 0.4$ N m and $T_\tau = 2.7$ N m.

As there is a gear box (ratio is 8) is mounted between the rotary damper and the scissors structure, the torque working

Figure 3. Test system for seat suspension.

on the scissors structure will be:

$$T = \begin{cases} 8T_{\tau} & \text{if } B \neq 0, \\ 8T_{\tau \mathrm{o}} & \text{if } B = 0. \end{cases} \tag{4}$$

The relationship between the MR damper torque and the vertical damping force working on seat suspension is essential to guide the seat suspension design. Figure 1 shows the geometry of the seat suspension and the relationship between the MR damper torque T and vertical damping force f_{MRF} can be obtained as:

$$f_{\mathrm{MRF}} = 2T/w = 2T/\sqrt{L_{\mathrm{o}}^2 - H^2}, \tag{5}$$

where L_{o} is the length of the beam of scissor structure, H is the height of the suspension. L_{o} is a constant value of 0.287 m, and H can be measured in real-time.

Thus the overall force generated by the seat suspension can be obtained by:

$$F_z = kx + f_{\mathrm{r}} + f_{\mathrm{MRF}}, \tag{6}$$

where k is the stiffness of the seat suspension, x is the displacement of the seat suspension, $f_{\mathrm{r}} = 64$ N is the friction force.

In summary, the above section provides the design principle which will offer useful guidelines for seat suspension design with a rotary MR damper. The comparison of the calculation pick force with the tested peak force is shown in figure 5.

3. The property test of the seat suspension and results discussion

3.1. Testing method

The dynamic properties of the seat suspension system are tested and evaluated in this section in terms of its field-dependent responses, amplitude, and frequency-dependent performance. In figure 3, the seat suspension was fixed onto a computer-controlled MTS machine (Load Frame Model: 370.02, MTS Systems Corporation), which was driven by a servo hydraulic system capable of exerting large axial loads onto the test specimen. The self-contained linear displacement transducer and load cells transmit the immediate responses of the tested specimen under harmonic excitations to the computer through a DAQ board. A DC power with two channels was ready to energize the magnetic fields of the specimen whenever needed. Once the testing started, the specimen moved in accordance with the preprogramed sinusoidal routine.

3.2. Test results

A series of experimental tests were conducted to evaluate and characterize the performance of this seat suspension using the above described experimental setup. For field-dependent tests, various harmonic inputs under different current levels, which are used to energize the magnetic field working on the MRF, were chosen to load this seat suspension. The properties of variable damping can be observed in figure 4(a). It can be seen that the force–displacement relationships form different parallelograms and the slopes of the parallelograms increase with the increasing current. It is also observed in figure 4(a) that the area of the force–displacement loops has a large increase before saturation occurs when the current level increases from 0 to 2 A with a step of 0.5 A. As the variation of damping is usually indicated by the area change of the enclosed force–displacement loops, the results demonstrate that this seat suspension shows controllable damping variations.

Figure 4(b) shows the responses of force–displacement when the seat suspension was loaded with sinusoidal signals with different amplitudes (1, 5, 10, and 15 mm) at constant frequency (1 Hz) and current (0 A). The effects of changing the amplitudes clearly show that the maximum force gains a large increase with the increasing amplitude. This set of results shows the amplitude-dependent properties of the tested seat suspension. Likewise, the effects of changing frequencies on the performance of the seat suspension are presented in figure 4(c). It can be seen that frequency variations have slight influence on the maximum force, the area of the loops, and the slopes of the parallelograms. In order to verify the correctness of the calculation in section 2.2, the comparison of the tested peak force and calculated peak force is presented in figure 5, where the tested peak force is obtained by using the peak force in figure 4(a) minus the preload force of 1045 N. The fitting result shown in figure 5 demonstrates the calculation method in section 2.2 accurately predict the dynamic performance of the seat suspension.

The above experimental results sufficiently verify that this proposed rotary MR damper has the same required properties as the linear MR dampers do while having some advantages that linear MR dampers do not possess. The compact design enables the rotary MR damper to be installed without any modifications to the original seat suspension structure and has further advantages in terms of weight reduction, smaller installation space, easy sealing and maintenance. Additionally, the rotary damper design improves the

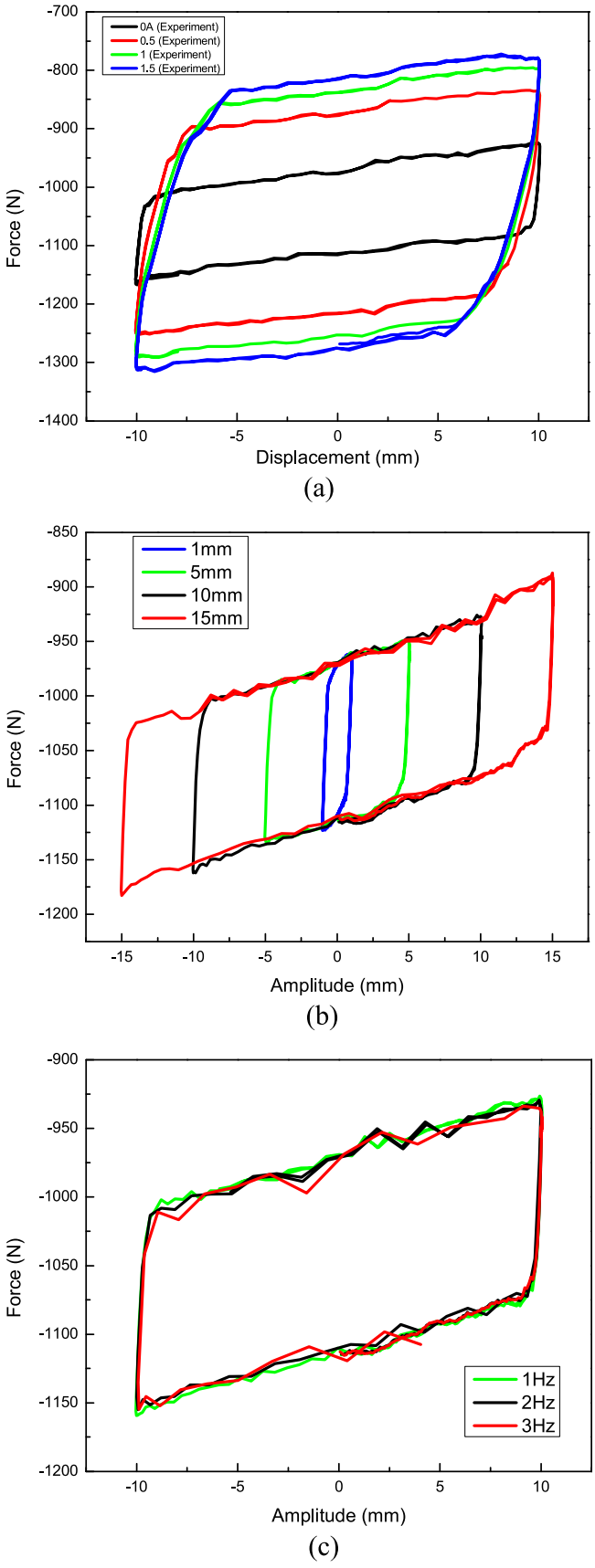

Figure 4. The test results of the seat suspension (a) different currents (b) different amplitudes (c) different frequencies.

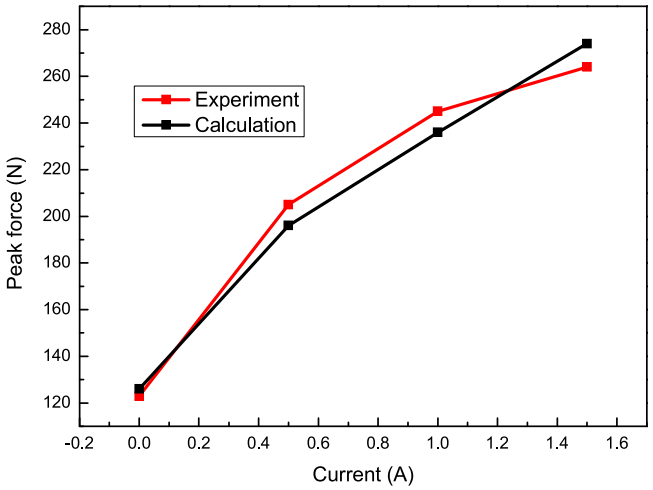

Figure 5. The comparison between the experimental peak force and calculated peak force.

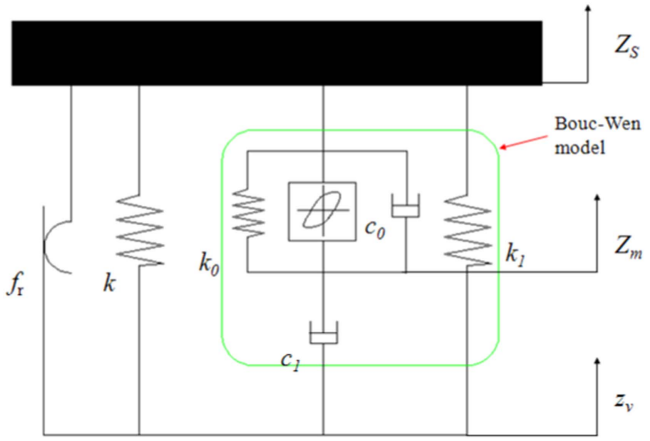

Figure 6. The mathematic model of seat suspension.

cost efficiency because it requires smaller quantity of MR fluid than linear MR dampers do.

4. Numerical effectiveness evaluation of the rotary MR seat suspension

4.1. The dynamic model of the seat suspension

Figure 6 shows the semi-active seat suspension model with stiffness k, friction f_r and the Bouc–Wen model for the MR damper. The suspension upper and base displacements are z_s and z_v, respectively. The governing equation of motion for the seat suspension is

$$m\ddot{z}_s + k(z_s - z_v) + f_r + f_{MRF} = 0, \quad (7)$$

where m is the total mass of a driver's body, seat suspension top platform and cushion. In this dynamic model, the overall force working on the seat suspension can be calculated by:

$$Fz = k(z_s - z_v) + f_r + f_{MRF}. \quad (8)$$

Based on the phenomenological model for magnetorheological dampers proposed by Spencer [24], the damping force

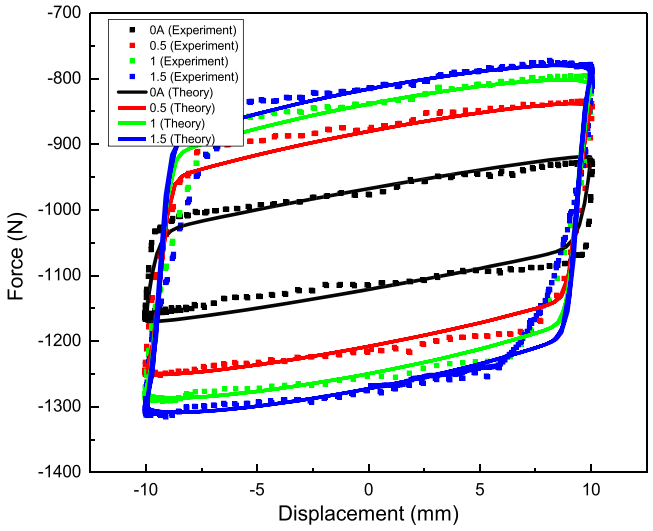

Figure 7. The fitting result of the mathematic model.

f_{MRF} can be obtained by the following equations:

$$\begin{aligned} f_{\mathrm{MRF}} &= c_1\dot{y} + k_1(x - x_0), \\ \dot{y} &= \frac{1}{c_o + c_1}[\alpha z + k_o(x - y) + c_o\dot{x}], \\ \dot{z} &= -\gamma|\dot{x} - \dot{y}||z|^{n-1}z - \mu(\dot{x} - \dot{y})|z|^n + A(\dot{x} - \dot{y}), \\ x &= Z_s - Z_v, \\ y &= Z_m - Z_v, \\ \alpha &= \alpha_a + \alpha_b I + \alpha_c I^2, \\ c_o &= c_{oa} + c_{ob} I + c_{oc} I^2, \\ c_1 &= c_{1a} + c_{1b} I + c_{1c} I^2, \end{aligned} \tag{9}$$

where I is the current applied to the MR damper. The parameters μ, γ, x_o, k_1, k_O, c_{oa}, c_{ob}, c_{oc}, A, n, α_a, α_b, α_c, c_{1a}, c_{1b}, and c_{1c} are used to characterize the MR damper. The optimized values for the parameters are determined by fitting the model to the experimental data obtained in the experiments. The least-square method in combination with the Trust-region-reflective algorithm available in MATLAB (R2013b) can be used for the parameter identification. The detailed parameter identification method has been given in our previous paper [25]. Figure 7 illustrates the tracing performance of the modelling results and experimental results and the identified parameters are shown in the table 3. It can be seen that the predicted data matches the experimental data very well.

4.2. Control algorithm

It is commonly recognized that the MR suspension system is difficult to model accurately because of its nonlinear and complicated nature. Many control algorithms have been investigated to control the MR dampers, including sliding mode control, robust control and fuzzy logic control [26–28]. As fuzzy logic control does not rely on the mathematical model of the full system, it is chosen to control MR damper in this study. The parameters of the dynamic seat model, shown in equation (6), are $m = 60\,\mathrm{kg}$, $k = 4100\,\mathrm{N\,m^{-1}}$. The input variables to the fuzzy controller are seat mass velocity V_s and relative velocity V_{rel} while the desired current is its output. The fuzzy logic control rules are based on the sky-hook strategy detailed as:

$$f_{\mathrm{MRF}} = \begin{cases} c_{\max} * V_{\mathrm{rel}} & V_s * V_{\mathrm{rel}} \geqslant 0, \\ c_{\min} * V_{\mathrm{rel}} & V_s * V_{\mathrm{rel}} < 0, \end{cases}$$

where the damping $c_{\max}$ is the on-state damping and $c_{\min}$ is the off-state damping. The on–off damping force is controlled by the sign of $V_s * V_{\mathrm{rel}}$. Based on the sky-hook control algorithm, the fuzzy logic control rules can be derived. The fuzzification of V_{rel} and V_s used in this research is NB, NS, ZE, PS and PB while the fuzzification of current is NB, NM, NS, ZE, PS, PM and PB. The fuzzy control rules are based on sky-hook control algorithm. For example, when the V_s and V_{rel} are NB, the output is maximum current which is corresponding to PB or NB in the fuzzy control algorithm. The other rules are designed following the same method. The final control rules are shown in table 4 [28]. It should be noted that the restriction of MR damper still exists in this study. Specifically, the MR damper should generate an active force in the same direction with relative motion when $V_s * V_{\mathrm{rel}} < 0$ in order to achieve better vibration control performance. The MR damper, however, can only generate a force in the opposite direction with the relative motion and as a result the current is set as zero when $V_s * V_{\mathrm{rel}} < 0$.

Table 3. The identified model parameters.

k_O	1500	A	2
k_1	700	n	2
x_o	0	α_a	89 839.1
γ	6e+5	α_b	205 322.1
μ	3e+6	α_c	−65 841
c_{oa}	198.1	c_{1a}	155 679.6
c_{ob}	635.6	c_{1b}	9.04705E+6
c_{oc}	−221.4	c_{1c}	−375 621.5

Table 4. The rules of the fuzzy controller.

	V_{rel}				
V_s	NB	NS	ZE	PS	PB
NB	PB	PM	PS	ZE	ZE
NS	PM	PS	ZE	ZE	ZE
ZE	PM	PS	ZE	NS	NM
PS	ZE	ZE	ZE	NS	NM
PB	ZE	ZE	NS	NM	NB

4.3. The numerical simulation results

4.3.1. The simulation results under harmonic excitation. In this test, the excitation, Z_v, is a sweep frequency signal with 10 mm amplitude. Its frequency linearly varies from 0.1 to 2.5 Hz in 25 s. The simulation results are shown in figure 8. Passive-off means that the rotary MR damper is out of control

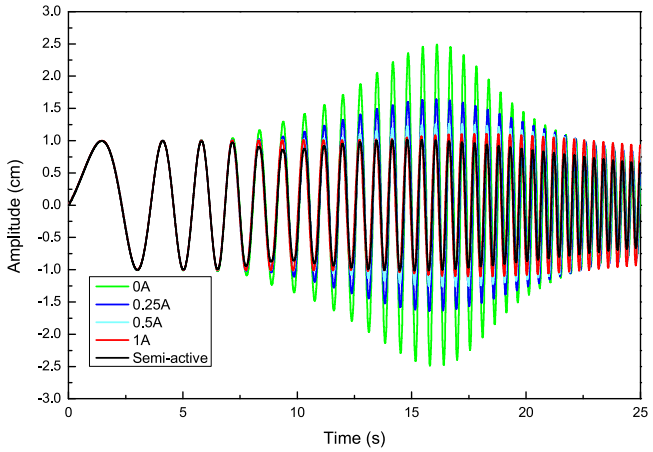

Figure 8. The simulation response of seat under harmonic excitation.

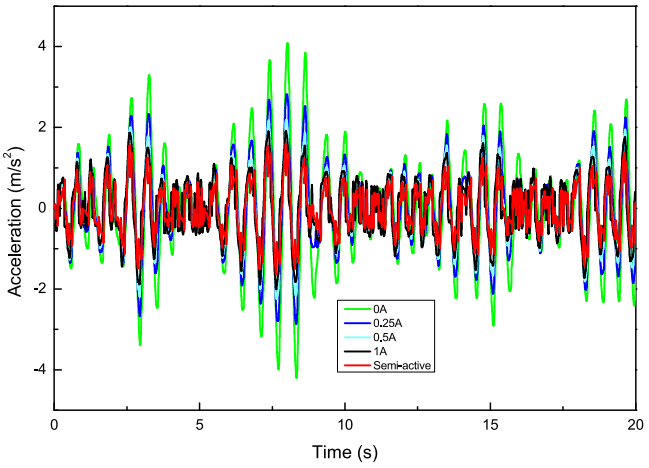

Figure 9. The simulation response of seat under random excitation.

because no control current was applied to it in this case. Passive-on refers to the situations where a certain current signal was chosen (0.25, 0.5, 1 A) to energize the rotary damper, and semi-active case means the rotary damper was under control of the fuzzy logic. It can be seen that the seat suspension with off state MR damper performs the worst and the resonance happens at around 16 s. On the contrary, the resonance peak is lower and lower with increasing current and can be barely seen for the seat suspension with 1 A current or controlled MR damper but it still can be observed that the semi-active seat suspension performs better than all the passive seat suspensions.

4.3.2. The simulation results under random excitation. The random excitation is generated by the following method. Firstly, the road displacement of the random ground surface [29, 30] can be defined as:

$$\dot{z}_{\mathrm{r}}(t) + \rho V z_{\mathrm{r}}(t) = V W_{\mathrm{n}}, \tag{10}$$

where ρ is the road roughness parameter, V is the vehicle speed, and W_{n} is white noise with intensity $2\delta^2\rho V$ in which δ^2 is the covariance of road irregularity. When the random ground profile is being generated, $\rho = 0.45\ \mathrm{m}^{-1}$, $\delta^2 = 300\ \mathrm{mm}^2$, and $V = 20\ \mathrm{m\ s}^{-1}$ are chosen. Then, a quarter car model is excited by this random ground surface and the response of the sprung mass will be used as the excitation for the seat suspension.

The simulation results are shown in figure 9 and it can be seen that the seat suspension with passive-off MR damper performs the worst and the controlled semi-active seat suspension performs the best.

5. Experimental effectiveness evaluation of the rotary MR seat suspension

5.1. Test system

The vibration isolation experiment was conducted to evaluate the effectiveness of the rotary MR damper to attenuate the vertical vibration. Two different excitations (constant frequency harmonic excitation and random road profile) were employed to evaluate the vibration reduction effectiveness of the proposed MR seat suspension. The experimental testing system is shown in figure 10. A normal commercial vehicle seat (GARPEN GSSC7) was fixed to the suspension system

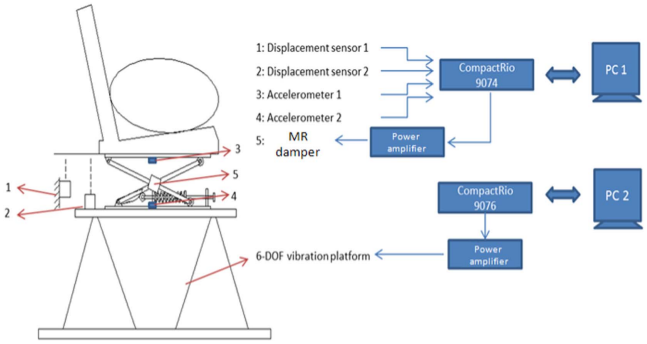

(a) Sketch

(b) Experiment

Figure 10. The effectiveness evaluation system for the seat vibration control.

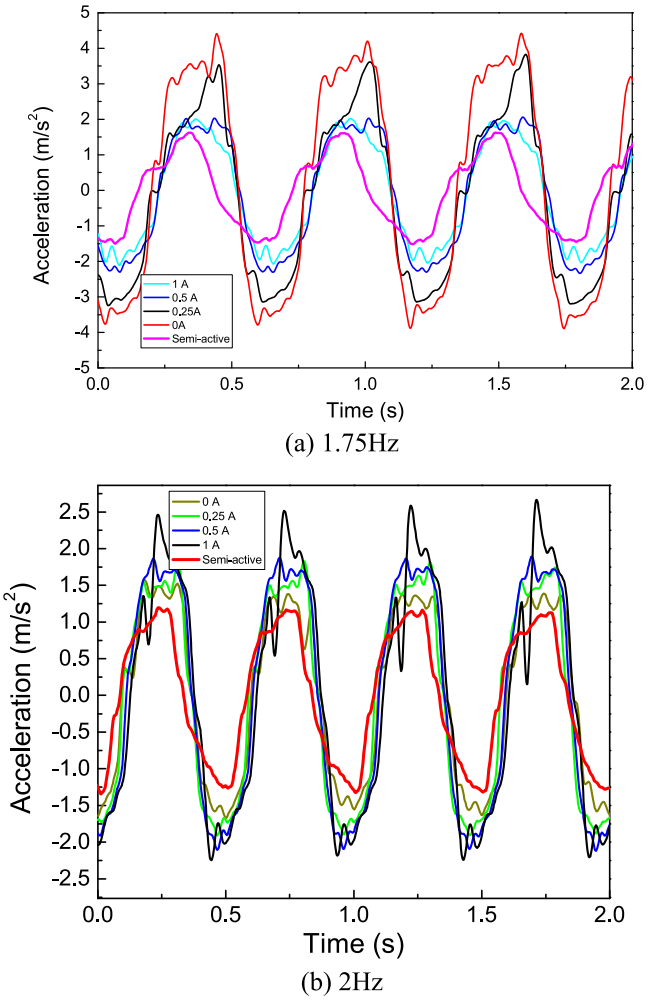

Figure 11. The test results of the MR seat suspension under harmonic excitation.

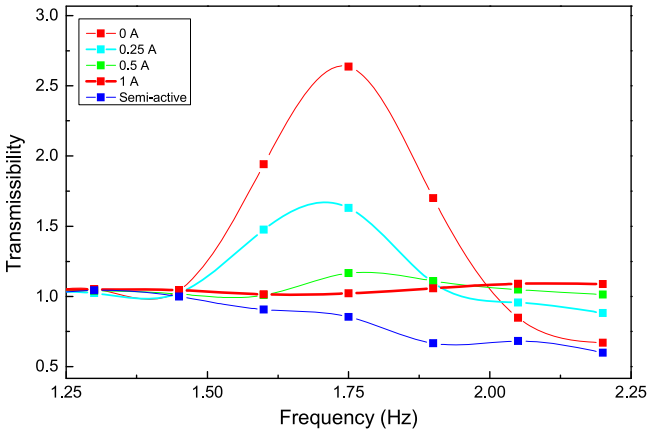

Figure 12. The transmissibility of the MR seat suspension under different frequencies.

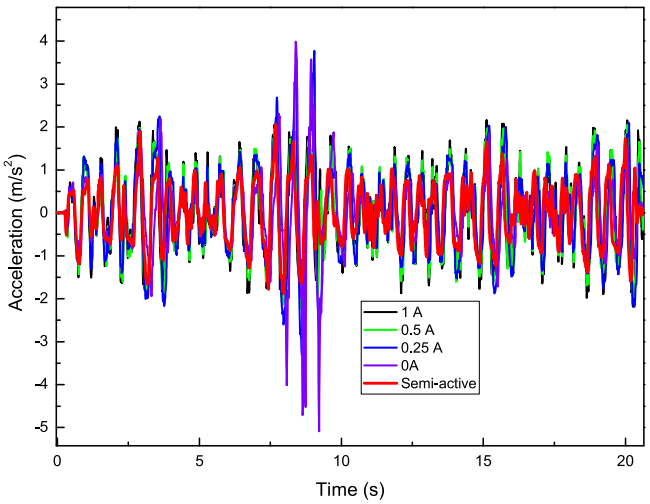

Figure 13. The performance of MR seat suspension under random excitation.

which was equipped with the rotary MR damper. The seat suspension system was driven to vibrate vertically by a vibration platform, as shown in figure 10. This vibration platform is controlled by NI CompactRio 9076. One displacement sensor (Micro Epsilon ILD1302-100) is installed on the bottom base of seat to measure the suspension relative displacement while the other displacement sensor (Keyence LB-11) was used to measure the seat's absolute displacement. Two accelerometers (ADXL203EB) were used to measure seat acceleration and excitation acceleration, respectively. Those measured signals were feedback to the seat suspension controller through a NI CompactRio 9074. The suspension controller then output a desired current signal. The current signal will be amplified by a power amplifier and then used to control the rotary damper.

5.2. Test results

5.2.1. The test results under harmonic excitation. In this test, different harmonic signals with different frequencies were used to excite the seat suspension. The responses of the seat suspension under two frequencies, 1.75 and 2 Hz, are given as representative examples. Figures 11(a) and (b) present the acceleration responses of the seat suspension under 1.75 Hz and 2 Hz, respectively. The performance of the seat suspension under passive-off (0 A), passive-on (0.25, 0.5, 1 A) and semi-active control cases were considered for each frequency testing. The comparison results between these cases are persuasive in terms of the performance of the semi-active rotary MR damper. Based on the testing results shown in figure 11, the semi-active case holds the minimum amplitude of the seat acceleration. The passive-off case performs worst when the excitation frequency is 1.75 Hz, however, it performs better than the passive-on cases when the excitation frequency is 2 Hz.

In order to further verify the vibration reduction effectiveness of the semi-active seat suspension, transmissibility was measured under different control cases. The transmissibility is defined as the ratio of the seat acceleration to the excitation acceleration. The smaller the ratio is, the more effective the suspension is. The experimental results, as shown in figure 12, verified that the semi-active case can

Table 5. The acceleration rms values.

	0	0.25 A	0.5 A	1 A	Semi-active
Experiment	1.023	1.050	0.803	0.871	0.621
Simulation	1.104	1.022	0.861	0.815	0.663

effectively reduce the transmissibility and performs the best over a large frequency range.

5.2.2. The test results under random excitation. Apart from the constant frequency excitation, random excitation was also used to test the seat suspension. Figure 13 shows the comparison of seat acceleration under passive-on cases (0.25, 0.5, 1 A), passive-off and semi-active control case. The acceleration amplitude under semi-active case is largely reduced compared to all passive-off and passive-on cases. A more direct comparison is given by calculating the rms under those three control cases. Both the rms values from the simulation and experimental results are given in table 5. Clearly, the semi-active control case has the smallest rms value, indicating that the rotary MR damper under fuzzy logic control has the most effective vibration reduction capability.

6. Conclusion

This paper proposes an innovative seat suspension design with a rotary MR damper, which can reduce not only the amount of MRF needed but also the sealing requirements. The testing results on the MTS machine show that it has the capability to vary damping in response to any change in current. Then an evaluation system is constructed, including the semi-active vehicle seat suspension, the control loop and vibration platform providing the excitations to this system. The vibration reduction effectiveness of the seat suspension is evaluated under two kinds of excitations, i.e. constant frequency excitation and random excitation. For both of the situations, the seat acceleration under fuzzy logic control holds the minimum value, which verified the semi-active rotary MR damper based seat suspension has the most effective vibration attenuation performance.

Acknowledgments

This research is supported by ARC Linkage Grants (LP160100132, No. 150100040), Open Research Fund Program of the State Key Laboratory of Advanced Design and Manufacturing for Vehicle Body, Hunan University (31515001) and the University of Wollongong and China Scholarship Council joint scholarships. The authors wish to gratefully acknowledge the help of Dr Madeleine Strong Cincotta in the final language editing of this paper.

References

[1] Burström L, Nilsson T and Wahlström J 2014 Whole-body vibration and the risk of low back pain and sciatica: a systematic review and meta-analysis *International Archives of Occupational and Environmental Health* pp 1–16
[2] Waters T, Genaidy A, Viruet H B and Makola M 2008 The impact of operating heavy equipment vehicles on lower back disorders *Ergonomics* **51** 602–36
[3] Bovenzi M 2010 A longitudinal study of low back pain and daily vibration exposure in professional drivers *Ind. Health* **48** 584–95
[4] Choi S B, Nam M H and Lee B K 2000 Vibration control of a MR seat damper for commercial vehicles *J. Intell. Mater. Syst. Struct.* **11** 936–44
[5] Sun S, Yang J, Deng H, Du H, Li W, Alici G and Nakano M 2015 Horizontal vibration reduction of a seat suspension using negative changing stiffness magnetorheological elastomer isolators *Int. J. Veh. Des.* **68** 104–18
[6] Wan Y and Schimmels J M 2003 Improved vibration isolating seat suspension designs based on position-dependent nonlinear stiffness and damping characteristics *J. Dyn. Syst. Meas. Control* **125** 330–8
[7] Maciejewski I, Meyer L and Krzyzynski T 2010 The vibration damping effectiveness of an active seat suspension system and its robustness to varying mass loading *J. Sound Vib.* **329** 3898–914
[8] Sun W, Li J, Zhao Y and Gao H 2011 Vibration control for active seat suspension systems via dynamic output feedback with limited frequency characteristic *Mechatronics* **21** 250–60
[9] Maciejewski I 2012 Control system design of active seat suspensions *J. Sound Vib.* **331** 1291–309
[10] Choi Y T and Wereley N M 2005 Mitigation of biodynamic response to vibratory and blast-induced shock loads using magnetorheological seat suspensions *Proc. Inst. Mech. Eng.* D **219** 741–53
[11] Choi S B and Han Y M 2007 Vibration control of electrorheological seat suspension with human-body model using sliding mode control *J. Sound Vib.* **303** 391–404
[12] Guo C, Gong X, Zong L, Peng C and Xuan S 2015 Twin-tube-and bypass-containing magneto-rheological damper for use in railway vehicles *Proc. Inst. Mech. Eng.* F **229** 48–57
[13] Sun S, Deng H, Li W, Du H, Ni Y Q, Zhang J and Yang J 2013 Improving the critical speeds of high-speed trains using magnetorheological technology *Smart Mater. Struct.* **22** 115012
[14] Sun S, Deng H and Li W 2014 A variable stiffness and damping suspension system for trains *Proc. SPIE* **9057** 90570P
[15] Carlson J D and Jolly M R 2000 MR fluid, foam and elastomer devices *Mechatronics* **10** 555–69
[16] Li W H, Du H, Chen G, Yeo S H and Guo N 2003 Nonlinear viscoelastic properties of MR fluids under large-amplitude-oscillatory-shear *Rheol. Acta* **42** 280–6
[17] Hu G, Ru Y and Li W 2014 Design and development of a novel displacement differential self-induced magnetorheological damper *J. Intell. Mater. Syst. Struct.* **26** 527–40
[18] Choi S B and Han Y M 2003 MR seat suspension for vibration control of a commercial vehicle *Int. J. Veh. Des.* **31** 202–15
[19] Choi Y T and Wereley N M 2005 Biodynamic response mitigation to shock loads using magnetorheological helicopter crew seat suspensions *J. Aircr.* **42** 1288–95
[20] Bai X X and Wereley N M 2014 Magnetorheological impact seat suspensions for ground vehicle crash mitigation *SPIE*

Smart Structures and Materials+ Nondestructive Evaluation and Health Monitoring

[21] Giorgetti A, Baldanzini N, Biasiotto M and Citti P 2010 Design and testing of a MRF rotational damper for vehicle applications *Smart Mater. Struct.* **19** 065006

[22] Nguyen Q and Choi S 2011 Selection of magnetorheological brake types via optimal design considering maximum torque and constrained volume *Smart Mater. Struct.* **21** 015012

[23] Zubieta M, Eceolaza S, Elejabarrieta M and Bou-Ali M 2009 Magnetorheological fluids: characterization and modeling of magnetization *Smart Mater. Struct.* **18** 095019

[24] Spencer B, Dyke S, Sain M and Carlson J 1997 Phenomenological model for magnetorheological dampers *J. Eng. Mech.* **123** 230–8

[25] Yang J, Du H, Li W, Li Y, Li J, Sun S and Deng H 2013 Experimental study and modeling of a novel magnetorheological elastomer isolator *Smart Mater. Struct.* **22** 117001

[26] Weber F 2015 Robust force tracking control scheme for MR dampers *Struct. Control Health Monit.* **22** 1373–95

[27] Weber F 2014 Semi-active vibration absorber based on real-time controlled MR damper *Mech. Syst. Signal Process.* **46** 272–88

[28] Yu M, Liao C, Chen W and Huang S 2006 Study on MR semi-active suspension system and its road testing *J. Intell. Mater. Syst. Struct.* **17** 801–6

[29] Choi S B and Kim W K 2000 Vibration control of a semi-active suspension featuring electrorheological fluid dampers *J. Sound Vib.* **234** 537–46

[30] Du H, Lam J, Cheung K, Li W and Zhang N 2013 Direct voltage control of magnetorheological damper for vehicle suspensions *Smart Mater. Struct.* **22** 105016